UNIVERSIDADE DE SÃO PAULO

INSTITUTO DE FÍSICA
CAIXA POSTAL 66318
05315-970 SÃO PAULO - SP
BRASIL

PUBLICAÇÕES

IFUSP/P-1277

J/ψ ELASTICITY DISTRIBUTION IN THE VECTOR DOMINANCE APPROACH

F.O. Durães[1], F.S. Navarra[1] and G. Wilk[1,2]

[1]Instituto de Física, Universidade de São Paulo

[2]Soltan Intitute for Nucleat Studies, Nuclear Theory Department
ul. Hoza 69, 00-681 Warsaw, Poland

Agosto/1997

Pág. 1-15

J/ψ Elasticity Distribution in the Vector Dominance Approach

F.O. Durães[1]*, F.S. Navarra[1]† and G. Wilk[1,2]‡
[1]*Instituto de Física, Universidade de São Paulo*
C.P. 66318, 05315-970 São Paulo, SP, Brazil
[2]*Soltan Institute for Nuclear Studies, Nuclear Theory Department*
ul. Hoża 69, 00-681 Warsaw, Poland

August 20, 1997

Abstract

The J/ψ elasticity distribution measured at HERA has been recently understood in terms of QCD models. We suggest that data can also be explained by the vector meson dominance mechanism supplemented by some hadronic description of energy loss, which is assumed to be provided by the Interacting Gluon Model (IGM).
PACS number(s): 13.85.Qk, 11.55.Jy

1 Introduction

At the HERA electron-proton collider the bulk of the cross section corresponds to photoproduction, in which a beam electron is scattered through a very small angle and a quasi-real photon (i.e. with Q^2 almost equal zero) interacts with the proton. For such small virtualities the dominant interaction mechanism takes place with the fluctuation of the photon into a hadronic state which interacts with the proton via strong force. High energy photoproduction therefore exhibits similar characteristics to hadron-hadron interactions. When the hadronic state in question is a vector meson this mechanism is known as the vector dominance model (VDM) [1] . The question that then arises is whether and when this hadronic state can be resolved in its constituent partons.

In the case of light vector mesons, the VDM hypothesis supplemented by a Regge theory of soft elastic vector meson interactions leads to the following behaviour of the production cross section

$$\sigma^{\gamma p \longrightarrow V p} \simeq W_{\gamma p}^{\delta} \tag{1}$$

where $W_{\gamma p}$ is the photon-proton center of mass energy and $\delta \simeq 0.22$. This prediction is supported by recent HERA measurements [2]. In the case of J/ψ a fit of data with eq. (1) gives $\delta \simeq 0.8 - 0.9$. A similar energy behaviour is observed in the inelastic J/ψ photoproduction ($\gamma + p \longrightarrow J/\psi + X$) cross section. In this reaction the energy scale is given by the large charm quark mass and perturbative QCD may be applied. Equivalently one may say that this particular photon fluctuation is a compact object, and one is in the short distance physics domain. Perturbative QCD (PQCD) models describe well the significant rise of the cross section with the photon-proton c.m.s. energy ($W_{\gamma p}$). Moreover these models can also reproduce the J/ψ momentum spectrum measured in inelastic J/ψ photoproduction. A very recent review of all these calculations can be found in ref. [3]. The emphasis of all these works is to determine with maximal confidence the J/ψ phase space region where PQCD is not only applicable but it is the only serious candidate to explain data. In this phase space region the dominant production process is boson-gluon fusion, $\gamma + g \longrightarrow J/\psi + X$. This reaction is particularly interesting because it allows a very good measurement of the gluon distribution in the proton.

In spite of the success of perturbative calculations some estimates of non-perturbative effects, like, for example, quark Fermi motion and hadronization effects (which may be treated in the context of non-relativistic QCD) have been presented. As a matter of fact, the mere existence of a hard scale in the problem does not authomatically exclude non-perturbative physics. In the much more studied case of J/ψ hadroproduction, after years of continuous improvements both in QCD calculations and experiments, the conclusion seems to be that perturbative theory is able to reproduce the main features of data but fails in some aspects, like the description of large x_F charm production and the magnitude of the integrated cross section [4]. In hadroproduction the situations where PQCD fails can be well understood, among other models, in terms of intrinsic charm [5]. The basic idea is that charm already pre-exists in the projectile as a virtual fluctuation. This notion is very close to the vector meson dominance picture and we would expect it to play some role also in charm photoproduction. The rise of the production cross section may be seen as a manifestation of PQCD but one might as well try to explain it (at least partially) with hadronic models, or, more precisely, with the help of VDM and some other hadronic theory of the process $J/\psi p \longrightarrow J/\psi p$ or $J/\psi p \longrightarrow J/\psi X$. Moreover, a stringent test of PQCD predictions requires a careful background subtraction of all the processes that contain a different physics. In the case of the J/ψ momentum spectrum such a background analysis was performed in refs. [6] and [7]. The analysis of ref. [7] was done with the help of Monte-Carlo implementations of models of diffractive production and production from "resolved photons". In this last production mechanism a gluon from the photon interacts with a gluon from the proton to produce a charm anti-charm pair. The conclusion was that, in the elasticity window $0.4 \leq z \leq 0.9$ ($z = E_\psi/E_\gamma$), the dominant production process is boson-gluon fusion. We believe that it is very important to extend the above mentioned background analysis and

*e-mail: dunga@uspif.if.usp.br
†e-mail: navarra@uspif.if.usp.br
‡e-mail: wilk@fuw.edu.pl

test other hadronic models giving special attention to the J/ψ z distribution. If it turns out that all reasonable models predict a wrong z spectrum this will leave PQCD as the only theoretical explanation of data in spite of the uncertainties in the overall normalization of the perturbative cross sections.

In this note we calculate the J/ψ z spectrum in the VDM approach. For the study of the energy flow in this particular meson-proton interaction we use the Interacting Gluon Model (IGM), which has been very successful in describing energy deposition and leading particle spectra in hadronic collisions (see for example [8, 9] and references quoted there). One advantage of using this model is that one can treat both diffractive and non-diffractive production mechanisms on the same footing.

2 VDM and IGM

In this section we briefly review some main ideas and formulas of the IGM. Before going into detail we emphasize that the application of the model to this situation is merely circumstantial. It is just a good model to represent hadron-hadron interactions and it is specially convenient here because of its ability to describe energy flow. We could, however, use other successful hadronic models as well. The main idea tested here is VDM.

In Fig. 1 we show schematically the VDM-IGM picture of a photon-proton collision. According to it, during the interaction the photon is converted into a hadronic (mesonic) state and then interacts with the incoming proton. The meson-proton interaction follows then the usual IGM picture, namely: the valence quarks fly through essentially undisturbed whereas the gluonic clouds of both projectiles interact strongly with each other (by gluonic clouds we understand a sort of "effective gluons" which include also their fluctuations seen as $\bar{q}q$ sea pairs). The meson looses fraction x of its original momentum and gets excited forming what we call a *leading jet* (LJ) carrying a fraction $1-x$ of the initial momentum. The proton looses a fraction y of its momentum [10]. Figs. 1a and 1b show inelastic non-diffractive (ND) events with J/ψ production. In Fig. 1a the J/ψ pre-exists as a photon fluctuation and after the interaction emerges as a leading particle (NDL). In 1b it is centrally (NDC) produced, i.e., it is formed in the central fireball together with other lighter particles as a result of multiple gluonic interactions. Figs. 1c, 1d, 1e and 1f show inelastic diffractive (D) events in which a rapidity gap is observed and in which presumably a "Pomeron" is emitted from the diffracted vector meson (DV), as in 1c and 1d or from the diffracted proton (DP) as in 1e and 1f. In 1c and 1e the J/ψ is the "diffractive leading particle" (DVL and DPL respectively) and in 1d and 1f it is diffractively and centrally produced (DVC and DPC respectively). For simplicity the vector meson V in Fig. 1 is here either a J/ψ or a ρ^0. We might also consider double Pomeron emission but, according to our knowledge on hadronic diffraction, these processes are strongly suppressed and their contribution to the cross section is one order of magnitude smaller than single diffractive processes.

The word "Pomeron" used above and graphically represented in Fig. 1 by the symbol $I\!P$ has the same meaning as in [8, 9] namely: in order to regard our process as being of the diffractive type we must assume that all gluons coming from the corresponding hadron have to form a colour singlet. Only then a large rapidity gap will form separating the diffracted hadron (the J/ψ in Fig. 1c ; the proton in Fig. 1e and 1f) and the diffractive system, which is the experimental requirement defining a diffractive event.

Otherwise a colour string would develop, connecting the diffracted proton and the diffractive cluster, and would eventually decay, filling the rapidity gap with produced secondaries. The Pomeron may be treated [11] as being composed of partons, i.e., gluons and sea $\bar{q}q$ pairs, in much the same way as hadrons, with some characteristic distribution functions, which are currently under investigation at HERA.

Our work is, in spirit, very close to ref. [6] and may be regarded to some extent as an update of that work to HERA with different inputs. It is possible to establish a correspondence between the main processes considered here and there (BI+TI = NDL+NDC+DVC ; BE+TI = DVL and BI+TE = DPL + DPC). The main difference is in the ingredients. In ref. [6] whenever $I\!P$ appears it is treated microscopically "a la" Donnachie-Landshoff and its gluons couple to the quarks either in the proton (in the $p-I\!P-p$ vertex) or in the J/ψ (in the $J/\psi-I\!P-J/\psi$ vertex). In our approach, in the latter vertex a Pomeron is emitted from the J/ψ gluonic cloud and the energy change of the J/ψ is described by the IGM formalism. Also, in ref. [6] inelastic (BI+TI) J/ψ production is treated with the color singlet (CS) model. We treat it with the IGM in which multiple gluon exchanges are included.

As discussed in ref. [8, 9], we start with the function $\chi(x,y)$, which describes the probability to form a central gluonic fireball (blobs in Fig. 1) , CF, carrying momentum fractions x and y of the two colliding projectiles:

$$\chi(x,y) = \frac{\chi_0}{2\pi\sqrt{D_{xy}}}\cdot \cdot\exp\left\{-\frac{1}{2D_{xy}}\left[\langle y^2\rangle(x-\langle x\rangle)^2+\langle x^2\rangle(y-\langle y\rangle)^2-2\langle xy\rangle(x-\langle x\rangle)(y-\langle y\rangle)\right]\right\} \quad (2)$$

In the above equation

$$D_{xy} = \langle x^2\rangle\langle y^2\rangle-\langle xy\rangle^2 \quad (3)$$

and

$$\langle x^n y^m\rangle = \int_0^{x_{max}} dx\, x^n \int_0^{y_{max}} dy\, y^m\, \omega(x,y). \quad (4)$$

Here χ_0 denotes the normalization factor provided by the requirement that $\int_0^1 dx\int_0^1 dy\,\chi(x,y)\theta(xy-K^2_{min}) = 1$ with $K_{min} = \frac{m_0}{\sqrt{s}}$ being the minimal inelasticity defined by the mass m_0 of the lightest possible central fireball CF.

In the above expressions, we specify the following interesting cases: I) $x_{max} = y_{max} = 1$ corresponds to Fig. 1a and 1b and the process is non-diffractive (ND); II) $x_{max} = x$ and $y_{max} = 1$ represents the emission of a Pomeron from the vector meson (DV), as shown in Fig. 1c and 1d; III) $x_{max} = 1$ and $y_{max} = y$ represents the emission of a Pomeron from the proton (DP), as in Fig. 1e and 1f. These upper cut-offs, $x_{max} = x$ and $y_{max} = y$ were not present in the non-diffractive formulation of the IGM. They are necessary to adapt the standard IGM to diffractive collisions. Each of them is kinematical restriction preventing the gluons coming from the diffracted hadron (and forming our object $I\!P$) to carry more energy than what is released in the diffractive system. The, so called, spectral function $\omega(x,y)$ contains all the dynamical inputs of the IGM in the general form given by (cf. [12])

$$\omega(x,y) = \frac{\sigma_{gg}(xyW^2)}{\sigma(W)}\, G(x)\, G(y)\, \Theta\left(xy-K^2_{min}\right), \quad (5)$$

where $G(x)$ and $G(y)$ denote the effective number of gluons in the meson and in the proton respectively. They are approximated by the respective gluonic structure functions. W is the photon-proton cm energy. σ_{gg} is the gluon-gluon cross section, which is computed over a wide range of scales given by xyW^2. Whenever the scale is larger than 2.3 GeV lowest order perturbative QCD formulas are used. Otherwise a parametrization which represents non-perturbative physics is employed. At the energies W considered here the bulk of the interaction happens in the non-perturbative domain. σ is the relevant meson-proton cross section or, in diffractive processes, the corresponding Pomeron-meson or Pomeron-proton cross section. The moments $\langle q^n \rangle$, $q = x, y$ (we only require $n = 1, 2$) are given by (4) and are the only places where dynamical quantities like the gluonic and hadronic cross sections appear in the IGM.

The ingredients used in eq. (5) will be different for each process depicted in Fig. 1.

In Fig. 1a the hadronic reaction is the inelastic $J/\psi - p$ scattering and therefore $\sigma = \sigma^{inel}_{J/\psi - p}$ and $G(x) = G^{J/\psi}(x)$. The charmonium-hadron cross section has been subject of intensive research in the context of nuclear physics and signatures of quark gluon plasma. Calculations seem to converge to $\sigma^{inel}_{J/\psi - p} \simeq 6 - 9$ mb [13]. We take this upper value. We shall assume that the gluon distribution has the same shape in all mesons, i.e., $G^{J/\psi}(x) = G^{\rho^0}(x) = G^{\pi}(x)$ and use, for the latter, the SMRS parametrization [14]. The specific shape chosen for these distributions, as it will be seen, does not affect much the results. Their normalization, however, plays a crucial role. We write the momentum sum rule for the gluon density $G^h(x)$ in hadron h as

$$\int_0^1 dx\, x\, G^h(x) = p^h \tag{6}$$

It is known that in a nucleon or in a light meson $p^h \simeq 0.5$, i.e., gluons carry half of the momentum of the hadron. The J/ψ, however, is a non-relativistic system and almost all its mass comes from the quark masses. The gluonic field, responsible for a weak binding, carries only a small fraction of the energy (and momentum) of the bound state. We expect therefore the normalization factor $p^{J/\psi}$ of $G^{J/\psi}(x)$ to be of the order of the energy stored in the field divided by the J/ψ mass :

$$p^{J/\psi} = \frac{M_{J/\psi} - 2\,m_c}{M_{J/\psi}} \simeq 0.033 \tag{7}$$

where m_c has been taken 1.5 GeV and $M_{J/\psi} = 3.1$ GeV.

In Fig. 1b $\sigma = \sigma^{inel}_{\rho^0 - p} \simeq \frac{2}{3}\sigma^{inel}_{p-p}$ where the last cross section is taken from data and $G(x) = G^{\rho^0}(x) = G^{\pi}(x)$ with $p^{\rho^0} = 0.5$.

In the diffractive processes of Figs. 1c and 1d the proton interacts with a Pomeron coming from a J/ψ and from a ρ^0 respectively. Therefore $\sigma = \sigma_{I\!P - p}$ and takes the same value no matter where $I\!P$ comes from. In order to make contact with the present knowledge about the Pomeron, we shall choose

$$\sigma(W) = = \sigma_{I\!P - p} = a + b \ln \frac{W^2}{W_0^2} \tag{8}$$

where $W_0 = 1\ GeV$ and $a = 2.6$ mb and $b = 0.01$ mb are parameters fixed from a previous [8] systematic data analysis of hadronic diffraction. The results obtained in [8] for $\sqrt{s}$ are here translated to the variable W. As it can be seen, $\sigma(W)$ turns out to be a very slowly varying function of W assuming values between 2.6 and 3.0 mb, which is a well accepted value for the Pomeron-proton cross section. The

function $G(x) = G^{I\!P}_h(x)$ represents the momentum distribution of the gluons belonging to the hadron subset called Pomeron and x is, in this case, the momentum fraction *of the hadron* carried by one of these gluons. We shall therefore use the notation $G^{I\!P}_{J/\psi}(x)$ and $G^{I\!P}_{\rho^0}(x)$ for processes of Figs. 1c and 1d respectively. This function should not be confused with the momentum distribution of the gluons inside the Pomeron, which in the literature is often called $f_{g/I\!P}(\beta)$. In a first approximation we shall take

$$G^{I\!P}_h(x) = p^{I\!P}_h (m+1)\frac{(1-x)^m}{x} \tag{9}$$

where m=5 and h is the hadron where the Pomeron comes from. As it was shown in ref. [9], the choice above corresponds for the function $f_{g/I\!P}(\beta)$ to a predominantly hard mixture between hard and soft Pomeron. The function above has the same shape for all hadrons, i.e., $G^{I\!P}_{J/\psi}(x) = G^{I\!P}_{\rho^0}(x) = G^{I\!P}_p(x)$. The normalization factor is different, however. We take $p^{I\!P}_{\rho^0} = p^{I\!P}_p = 0.05$. This same expression has already been used by us recently [8] in an analysis of hadronic diffraction where this last parameter was fixed. This number can be interpreted as follows. In an usual hadron (nucleon or light meson) gluons carry 0.5 of the total momentum and the gluonic cluster constituting the Pomeron carries 0.1 of the total gluonic momentum. Therefore the gluons of the Pomeron carry, on the average, $0.1 \times 0.5 = 0.05$ or 5% of the total hadron momentum. Using the same reasoning for the J/ψ we find that, when the heavy meson emitts a Pomeron, the corresponding bunch of gluons carries $0.1 \times 0.033 = 0.0033$ or 0.33% of the total J/ψ momentum. We have then $p^{I\!P}_{J/\psi} = 0.0033$. We insist on this point because this is the main difference between ordinary hadrons and heavy mesons in the IGM. This difference qualitatively explains why heavy mesons emerge from the collision faster than other particles. Because they contain less energetic gluons they can not loose much energy. The diffractive interaction (with $I\!P$ emission) amplifies this effect.

Finally in the diffractive processes 1e and 1f a Pomeron coming from the proton interacts with the J/ψ and ρ^0 respectively. We have then $\sigma = \sigma_{I\!P - J/\psi}$ and $G(x) = G^{J/\psi}(x)$ in 1e and $\sigma = \sigma_{I\!P - \rho^0}$ and $G(x) = G^{\rho^0}(x)$ in 1f. In both cases $G(y) = G^{I\!P}_p(y)$. The Pomeron-hadron cross sections $\sigma_{I\!P - J/\psi}$, $\sigma_{I\!P - \rho^0}$ are unknown. We shall assume that $\sigma_{I\!P - \rho^0} = \frac{2}{3}\sigma_{I\!P - p}$ and $\sigma_{I\!P - J/\psi} = \frac{1}{4}\sigma_{I\!P - p}$.

3 J/ψ spectra

As mentioned before J/ψ's can be produced either centrally (C) or as leading particles (L). Their momentum spectra are thus labeled F_C and F_L respectively. Moreover they can be produced diffractively (D) or non-diffractively (ND). We have thus four contributions to the final J/ψ fractional momentum (or elasticity z) distribution which are called F^{ND}_C, F^{D}_C, F^{ND}_L and F^{D}_L. The two diffractive distributions can be further splitted into four according to whether the Pomeron comes from the vector meson (DV) or whether it comes from the proton (DP) giving : F^{DP}_C, F^{DV}_C, F^{DP}_L and F^{DV}_L. They can be explicitely written in terms of the function $\chi(x,y)$ as:

$$F^i_C(z) = \int_0^1 dx \int_0^1 dy\ \chi^i(x,y)\,\delta(z - x + y)\,\Theta\left(xy - \frac{M^2_{J/\psi}}{W^2}\right) \tag{10}$$

and

$$F^i_L(z) = \int_0^1 dx \int_0^1 dy\ \chi^i(x,y)\,\delta(z - 1 + x)\,\Theta\left(xy - \frac{m_0^2}{W^2}\right)\,\Theta\left[y - \frac{(M_{J/\Psi} + m_0)^2}{W^2}\right] \tag{11}$$

$$= \int_{y_{min}}^{1} dy\, \chi^i(x = 1 - z; y)$$

with

$$y_{min} = Max\left[\frac{m_0^2}{(1-z)W^2}, \frac{m_0^2}{(M_{J/\Psi}+m_0)^2}\right] \qquad (12)$$

where $z = \frac{E_{J/\Psi}}{E_\gamma}$ is the J/Ψ energy fraction (which in the IGM where all masses have been consistently neglected [12, 8] coincides with the momentum fraction). The superscript i = ND, DV or DP indicates that the first, the second or the third line in Fig. 1 is considered. Notice that, when dealing with the leading particle spectra, we have to introduce the additional kinematical constraint, $y > \frac{(M_{J/\Psi}+m_0)^2}{W^2}$, which ensures that the mass M_X ($M_X = \sqrt{y}W$, see Fig. 1) is large enough to produce both the measured J/Ψ particle of mass $M_{J/\Psi}$ and the minimal CF of mass m_0, as demanded by the IGM. Having defined all the constants and parameters that are needed we plot the six curves F_C^{ND}, F_C^{DV}, F_C^{DP}, F_L^{ND}, F_L^{DV} and F_L^{DP} in Fig. 2 in arbitrary units. The three central curves are represented with dashed lines whereas the leading ones with solid lines. As expected, central production gives origin to slower J/ψ's and leading production generates faster J/ψ's. Among the leading curves we observe that when the J/ψ emitts a Pomeron there is a peak around $z \simeq 1$. This is expected since $I\!P$ emission implies a very small energy loss. F_L^{DV} is thus harder than F_L^{ND} and F_L^{DP}. The behaviour of the three central curves can be understood in the following way. The non-diffractive distribution defines the main features of central production in the IGM. Our broad curve is in sharp contrast with the "resolved photon" distribution presented in refs. [7, 15] (which has a peak at $z \to 0$). The relevant process there is $g + g \to c\bar{c}$, which gives a very soft $c\bar{c}$ momentum distribution. This is a consequence of the softness of gluon distributions. In the IGM multiple gluon emission (or radiation) makes possible larger energy momentum release in the central fireball and consequently faster $c\bar{c}$ pairs may be formed. This point was extensively discussed in [16]. In the DV process there will be a gap separating the fast leading light vector meson and J/ψ. This rapidity separation prevents the J/ψ from having very large z values. Therefore the F_C^{DV} curve dies faster than F_C^{ND} at large z. In the DP case there is a gap between the J/ψ and the proton. This forces the J/ψ to move closer to the leading vector meson. The distribution F_C^{DP} will thus favour larger values of z than F_C^{ND}.

4 Comparison with experimental data

The data from ref. [7] were presented in two samples. The first one included J/ψ's with all values of transverse momentum p_T and the second contained only J/ψ's with $p_T^2 \geq 1(GeV/c)^2$. This last data sample was expected to exclude soft and diffractive processes being thus appropriate for a PQCD description, which was indeed successful (cf. ref. [3]). We start adressing the minimum bias sample which presumably has stronger non-perturbative (hadronic) effects. All the diagrams in Fig. 1 must be included. Unfortunately we are not able to calculate the relative weigth of each of the six distributions. Based on what is known from usual hadronic collisions we expect the non-diffractive contributions to be dominant. More specifically we expect F_C^{ND} to be the dominant curve at lower values of z ($z \leq 0.5$) and we expect F_L^{ND} to dominate the total spectrum in the region $0.5 \leq z \leq 0.9$. For $z \geq 0.9$ data

suggest the existence of a peak which in our model is most naturally described by F_L^{DV}. In order to test these conjectures we adjust, in Fig. 3, F_C^{ND} (dashed line), F_L^{ND} (dot-dashed line), and F_L^{DL} (dotted line) to the data points in the z regions where they should work best. Although we do not know exactly how to combine these individual contributions in our model, we can use information from the FTPS experiment [17]. This collaboration has measured separately the following four contributions: elastic, photon dissociation into $J/\psi + X$ (equivalent to our F_L^{DP}), photon dissociation with a J/ψ isolated in rapidity (our F_L^{DV}) and inclusive J/ψ production without rapidity gaps (corresponding to the sum $F_L^{ND} + F_C^{ND}$). Apart from constant factors we may extract the relative weigths from the corresponding cross sections identifying $\sigma(\gamma p \longrightarrow J/\psi_{diff} + X) = 4.4 \pm 0.9$ nb with the weigth of the integrated F_L^{DV} spectrum and $\sigma(\gamma p \longrightarrow J/\psi + X) = 5.1 \pm 1.3$ nb with the weigth of the sum $F_C^{ND} + F_L^{ND}$. The resulting relative weigths are 0.27,0.27 and 0.46 for F_C^{ND}, F_L^{ND} and F_L^{DV}, respectively. The final spectrum with these weigths is shown in Fig. 3 with dot-dashed line labeled II. The solid line (labeled I) shows a combination of the three distributions with equal weigths for F_C^{ND}, F_L^{ND} and F_L^{DV}. Both choices agree nicely with data within the error bars.

In Fig. 4 we compare the data sample of $p_T^2 \geq 1GeV^2$ and $0.4 \leq z \leq 0.9$ with F_L^{ND}, which is expected to be the dominant IGM contribution in this region. In order to take the minimum transverse momentum into account we replace $M_{J/\psi}$ by $M_T = \sqrt{M_{J/\psi}^2 + p_T^2}$ in eqs. (11) and (12). As it can be seen the agreement is very good.

In Fig. 5 we make the same type of comparison as in Fig. 3 between our model and lower energy data from the FTPS collaboration [17]. All the five curves have the same meaning as in Fig. 3. The only difference is that now they are computed at $E_\gamma = 150$ GeV. Data from NMC and NA14 experiments are also shown in the figure.

5 Summary and conclusions

In this note we have suggested that, in close analogy to what happens in charm hadroproduction, a visible part of experimental data is not described by PQCD. There is room for hadronic (non-perturbative) effects. One way to treat them is with the vector meson dominance mechanism plus some description of the meson-proton interaction. The energy flow (and consequently the J/ψ spectrum) in these reactions is well understood in the context of the IGM. The comparison with data presented in Figs. 3 and 4 shows a good agreement. Of course we do not consider this result as the final word, since we know that PQCD must be included, but rather as an indication that a hadronic theory of energy loss is compatible with data and may be visible. In our model there are PQCD interactions between gluons in the gluonic clouds but the charmed quarks do not interact in this regime. The fact that F_L^{ND} agrees so well with data in Fig. 4 indicates that large z events may be interpreted as "peripheral" $J/\psi - p$ collisions in which the small amount of gluons in the J/ψ is not enough to stop it. We obtain thus fast leading particles.

Acknowledgements: This work has been supported by CNPq and FAPESP under contract number 93/2463-2. We would like to warmly thank E. Ferreira and R. Covolan for many fruitful discussions. GW would also like to thank IFUSP for warm hospitality extended to him during his visit there.

References

[1] S.D.Holmes, W. Lee, J.E. Wiss, *Ann. Rev. Nucl. Part. Sci.* , **35** (1985) 397 ; T.H. Bauer, R.D. Spidal, D.R. Yennie , F.M. Pipkin, *Rev. Mod. Phys.* **50** (1978) 261; J.Sakurai, *Ann. Phys.* **11** (1960) 1 and *Phys. Rev. Lett.* **22** (1969) 981.

[2] For a recent review see, for example, N. Cartiglia, *Diffraction at HERA*, hep-ph/9703245 - talk given at the SLAC Summer School 1996.

[3] Cf., for example, P.Hoyer, *Charmonium production at ELFE energies*, talk given at the *Second ELFE Workshop*, Saint Malo, Sept. 23-27, 1996 (hep-ph/9702385) and references therein; M. Kramer, *Nucl. Phys.* **B459** (1996) 3; M. Cacciari and M. Kramer, *Phys. Rev. Lett.* **76** (1996) 4128.

[4] P.E. Karchin, *Hadroproduction of Charm and Beauty*, hep-ph/9703331 - to appear in the Proc. of the XVI Int. Conf. on Physics in Collisions, Mexico City, 1996.

[5] R. Vogt, *Nucl. Phys. (Proc. Suppl.)* **55A** (1997) 135 and references therein; G. Ingelman and M. Thunman, *Z. Phys.* **C73** (1997) 505 and references therein; S.J. Brodsky, P. Hoyer, C. Peterson and N. Sakai, *Phys. Lett.* **B93** (1980) 451; S.J. Brodsky, C. Peterson and N. Sakai, *Phys. Rev.* **D23** (1981) 2745.

[6] H. Jung, G.A. Schuler and J. Terron, *Int. Jour. Mod. Phys.* **A7** (1992) 7955.

[7] S.Aid et al., (H1 Collab.), *Nucl. Phys.* **B472** (1996) 3 (hep-ex/9603005); M.Derrick et al. (ZEUS Collab.), *Phys. Lett.* **B350** (1995) 120.

[8] F.O.Durães, F.S.Navarra and G.Wilk, *Phys. Rev.* **D55** (1997) 2708 and references therein.

[9] F.O.Durães, F.S.Navarra and G.Wilk, "Diffractive Mass Spectra at HERA in the Interacting Gluon Model", IFUSP Report IFUSP/P-1260 (1997).

[10] It can be also deflected with some invariant momentum transfer t. However, because the IGM does not include so far any transverse momentum transfers, the results presented here must be regarded as appropriately averaged/integrated over t.

[11] G.Ingelman and P.Schlein, *Phys. Lett.* **B152** (1985) 256; A.Donnachie and P.V.Landshoff, *Phys. Lett.* **B191** (1987) 309; *Nucl. Phys.* **B303** (1988) 634.

[12] F.O.Durães, F.S.Navarra and G.Wilk, *Phys. Rev.* **D47** (1993) 3049.

[13] D. Kharzeev and H. Satz, *Phys. Lett.* **B366** (1996) 316; **B356** (1995) 365; **B334** (1994) 155.

[14] P.J. Sutton, A.D. Martin, R.G. Roberts and W.J. Stirling, *Phys.Rev.* **D45**, (1992) 2349.

[15] L.P.A. Haakman, A.B. Kaidalov and J.H. Koch, "Charm production in deep inelastic and diffractive scattering", Report NIKHEF 97-015; hep-ph/9704203.

[16] F.O.Durães, F.S.Navarra, C.A.A. Nunes and G.Wilk, *Phys. Rev.* **D53** (1996) 6136.

[17] B.H. Denby et al. *Phys. Rev. Lett.* **52** (1984) 795.

Figure Captions

Fig. 1 IGM description of a photon-proton scattering with J/ψ production. a) non-diffractive leading production; b) non-diffractive central production; c) diffractive production with Pomeron emission from the J/ψ; d) central diffractive production with Pomeron emission from the light vector meson (V); e) leading diffractive production with Pomeron emission from the proton; f) central diffractive production with Pomeron emission from the proton.

Fig. 2 Individual contributions of the six processes of Fig. 1 to the J/ψ z spectrum.

Fig. 3 Comparison of the IGM distributions F_C^{ND} , F_L^{ND}, F_L^{DV} and their sum (curves I and II) with data from ref. [7]. Curves I and II represent the combination of F_C^{ND}, F_L^{ND} and F_L^{DV} with weigths 0.27, 0.27, 0.46 and 0.33, 0.33, 0.33 respectively.

Fig. 4 Comparison of the IGM distribution F_L^{ND} with data of ref. [7] with restricted acceptance $p_T^2 \geq 1\,(GeV/c)^2$ and $0.5 \leq z \leq 0.9$.

Fig. 5 Comparison of the IGM distributions F_C^{ND} , F_L^{ND}, F_L^{DV} and their sum (curves I and II) with data from ref. [17]. I and II have the same meaning as in Fig. 3.

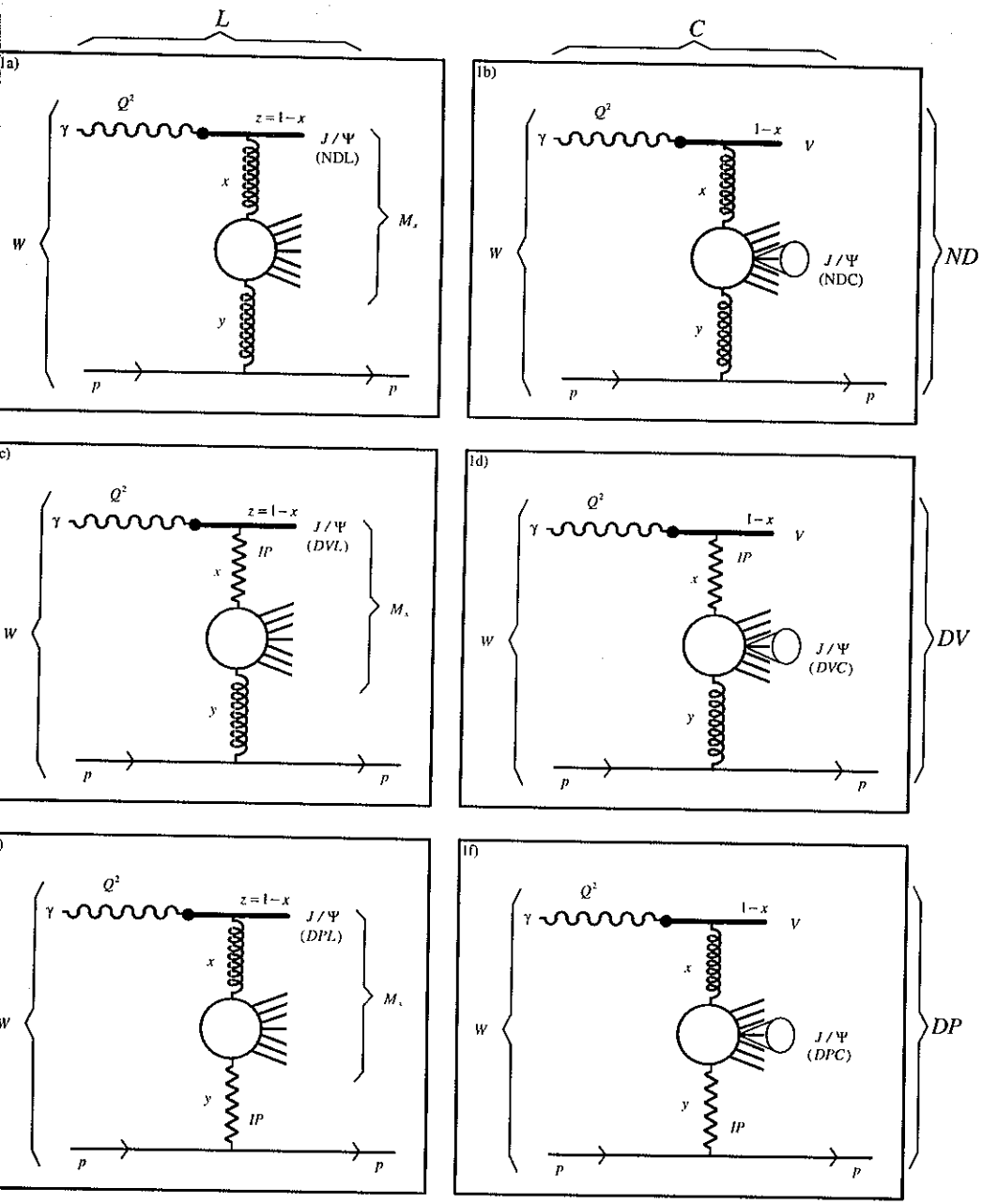

Figure 1

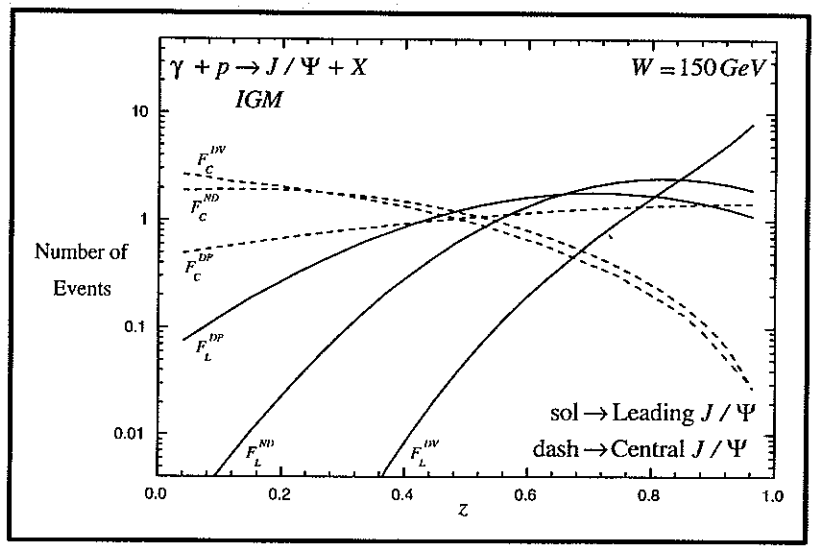

Figure 2

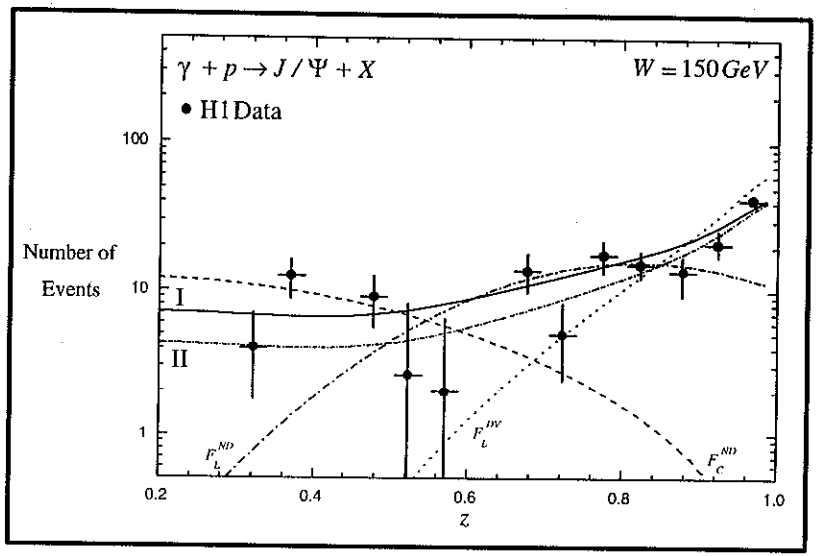

Figure 3

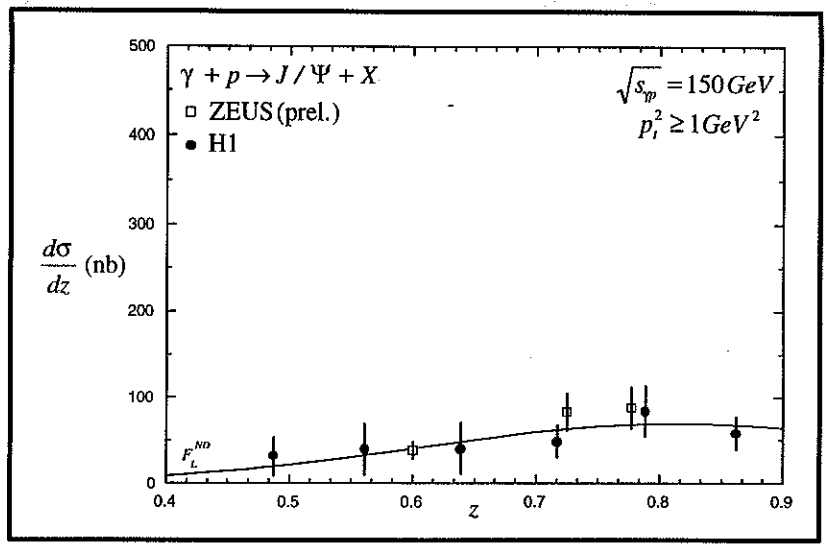

Figure 4

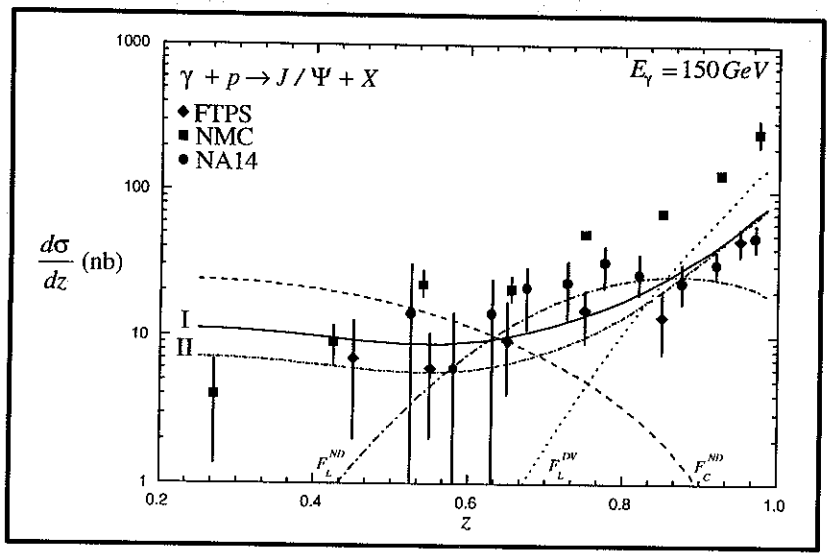
$\gamma + p \to J/\Psi + X$
$E_\gamma = 150\,GeV$
FTPS
NMC
NA14
$\frac{d\sigma}{dz}$ (nb)
I
II
F_L^{ND}
F_L^{DV}
F_C^{ND}
1000
100
10
1
0.2
0.4
0.6
0.8
1.0
z

Figure 5